Spectroscopic investigation of historical uranium glasses

CALAS, Georges, GALOISY, Laurence, HUNAULT, Myrtille, RAUTIYAL, Prince, SKERRAT-LOVE, Katrina, RIGBY, Jessica and BINGHAM, Paul <http://orcid.org/0000-0001-6017-0798>

Spectroscopic investigation of historical uranium glasses

Georges Calas[1], Laurence Galoisy[1], Myrtille O.J.Y. Hunault[2], Prince Rautiyal[3], Katrina Skerratt-Love[3], Jessica Rigby[3], Paul A. Bingham[3]

[1] Institut de Minéralogie, de Physique des Matériaux et de Cosmochimie (IMPMC), Sorbonne Université, CNRS, Muséum National d'Histoire Naturelle, IRD, 75005 Paris, France

[2] Synchrotron SOLEIL, L'Orme des Merisiers, Saint Aubin BP 48, 91192 Gif-sur-Yvette, France

[3] Materials and Engineering Research Institute (MERI), Sheffield Hallam University, City Campus, Howard Street, Sheffield S1 1WB, UK

** Corresponding author: georges.calas@sorbonne-universite.fr (G. Calas).*

Keywords: uranium; glasses; cultural heritage; conservation science; optical spectroscopy; XANES electron paramagnetic resonance (EPR); HERFD-XANES; Colour technology

Highlights:

- Spectroscopic study of two "Art Nouveau" and "Art Déco" glasses coloured by uranium
- Glass colouration and radiation-induced defects are investigated by spectroscopic methods
- Optical absorption and HERFD-XANES spectroscopy show mainly uranyl (UO_2^{2+}) contributions
- The oxidation state of uranium was controlled by the use of As and Sb as oxidizing agents
- Absorption properties of penta- and hexavalent uranium are discussed.
- The presence of multivalent elements reduces the concentration of defect centres

ABSTRACT

We present spectroscopic investigations of uranium in two historical glasses. A 1920's-1930's Art Deco (Bagley Carnival) green soda-lime-silica uranium glass bowl and a 1930's-1940's (Thomas Webb) yellow full lead crystal uranium glass vase were studied using optical absorption spectroscopy, XRF and SEM-EDX, X-band EPR and Uranium speciation may be different in the two glasses. Uranium occurs as uranyl groups (UO_2^{2+}) with minority reduced uranium species, mostly as U(V), more important in the Webb glass than in the Bagley glass. The differences between the two glasses arise from the fining procedure and result from the presence of other multivalent elements and differences in base glass composition. Electron Paramagnetic Resonance (EPR) spectra show the presence of an incipient signal close to g~2, partially annealed by heating to 550°C, which we assign to a small concentration of radiation-induced defects caused by uranium decay. The presence of multivalent glass components in addition to U (As + Cu + Fe in the Bagley glass and Sb + Fe in the Webb glass) can trap the electron–hole pairs generated by the presence of uranium. This may explain the weakness of this signal in these glasses that anyway received a limited radiation dose since their fabrication. The low activity of these glasses, close to the background radiation, confirms that there is no danger to exhibiting them in museums.

1. INTRODUCTION

Before Eugène Péligot isolated uranium metal in 1841, pitchblende was already extracted from the Habsburg silver mines in Joachimsthal, Bohemia, and used as a colouring agent in the local glassmaking industry from the early 19th Century to the first half of the 20th Century [1,2]. Uranium glasses were then elaborated, mostly for glassware and decorative purposes: vases, drinking vessels, stained glasses and even jewellery. Yellow and green vivid colours were obtained by incorporating U(VI) oxides such as $Na_2U_2O_7$, $K_2U_2O_7$ and $(NH_4)_2U_2O_7$ in the raw materials [3]. During glassmaking, the colour was controlled by adjusting the oxidation state of uranium and via the addition of complementary colouring constituents (e.g. certain transition metals). Indeed, as U(IV) imparts a deep green colour to silicate glasses, U(VI) gives a bright yellow colour [1]. The intermediate oxidation number U(V) is not an efficient colouring agent because most optical transitions occur in the near infrared (NIR) [4]. A green colour of U(VI) glasses may also be obtained by incorporating Cu^{2+}. The use of uranium as a colouring agent was

particularly popular during the "Art Nouveau" and "Art Déco" periods in Europe, USA, and Japan [5]. However, restrictions were placed on the use of uranium in 1942 for the purposes of World War II and uranium glasses were no longer produced. Nowadays, there is a concern about a possible exposure of the public to ionizing radiations emitted by uranium-containing glasses in museums and private collections [3]. An additional environmental concern is raised by the management of glass dumpsites, with the recent evidence of the contribution of various isotopes (mostly ^{40}K, but also ^{210}Pb from Pb chemicals and from the decay of ^{238}U) to the radioactivity of ordinary glass waste [6]. There is also a recent interest for using the radiation defects in window glasses, screens of mobile phones, etc., in order to track the radiation history of the general population [7,8]. In addition, uranium glasses remain of interest to collectors, as well as historians and scientists [3,5].

The goal of this study was to investigate uranium contents and speciation in these glasses, and to ascertain whether these parameters -i.e. oxidation state, coordination number and site geometry - are at the origin of the different colours of these historical glasses. Another goal was to evidence whether these two glasses suffered detectable radiation damage after 80-100 years as a consequence of the presence of uranium in their structure. Whereas considerable research has been published on uranium in glasses of technological interest for the immobilisation of nuclear wastes [9-12], little has been reported on decorative glass objects such as those studied here. However, historical uranium glasses may provide useful information, not only on these glasses, their methods of production and their properties, but also to the nuclear waste immobilisation community, since these are synthetic uranium-bearing silicate glasses with ages of up to ~150 years which predate radioactive waste glass research by many decades in some cases.

For this study, uranium speciation and radiation damage have been investigated in two uranium containing historical pieces: a 1920's-1930's Art Deco uranium green glass, the "Carnival glass" manufactured by Bagley's Glassworks in Knottingley, England, and a 1930's-1940's yellow uranium glass vase manufactured by Thomas Webb & Sons glass company in Stourbridge, England (Fig. 1). Both glasses glow strongly under UV light. Since both glasses are of a broadly similar age (Bagley ~90-100 years; Webb ~80-90 years). Glass compositions were investigated using XRF (Bagley) and SEM-EDX (Webb). Glass colour and uranium speciation were investigated by UV-visible-near infrared optical absorption spectroscopy and High-Energy Resolution Fluorescence-Detected (HERFD) X-ray Absorption Near-Edge Structure (XANES). Paramagnetic components and any

radiation damage were investigated using X-band Electron Paramagnetic Resonance (EPR) spectroscopy.

Figure 1. Left: Bagley Carnival uranium glass bowl. Right: Thomas Webb yellow uranium glass vase.

2. RESEARCH AIMS

The aim of the present study was to understand the nature, composition, oxidation states and colour / optical absorption of two historical glasses coloured by uranium and the impact of their radioactivity during display in museums. Whilst the radioactivity and colour of historical glasses has received some attention (see Section 1), further research can provide additional insight on U-speciation in glasses. In addition, historical glasses coloured by uranium can also provide useful insight for researchers studying the impact of radionuclides on the glasses now being used globally for the immobilisation of radioactive wastes, for example in terms of redox behaviour and radiation-induced defects.

The chemical compositions of the two glasses studied here, as determined by XRF and SEM-EDX, are representative of 1920's-1930's Art Deco (Bagley Carnival, a green soda-lime-silica uranium glass) and 1930's-1940's (Thomas Webb, a yellow full lead crystal uranium glass). The origin of their colouration was studied by optical absorption spectroscopy and High-Energy Resolution Fluorescence-Detected (HERFD)-XANES. Uranium occurs as uranyl (UO_2^{2+}) with minority U(V). The difference between the colours of the two glasses arises from different base glass composition, including U-concentration and the presence of other multivalent elements, and different fining procedures. Electron Paramagnetic Resonance (EPR) spectra show the presence of an incipient signal, assigned to a small concentration of radiation-induced defects. The presence of multivalent glass components that can trap the electron–hole pairs generated during uranium decay may

explain the weakness of this signal in these glasses that anyway received a limited radiation dose. The low activity of these glasses, close to the background radiation, confirms that there is no danger to exhibiting them in museums.

3. EXPERIMENTAL PROCEDURES

Chemical compositions of the two glass samples were studied (i) for the Bagley Carnival glass using X-ray fluorescence (XRF) spectroscopy; and (ii) for the Thomas Webb glass using Scanning Electron Microscopy – Energy Dispersive X-Ray Spectroscopy (SEM-EDX). This was due to the need to avoid preparing powdered samples of the higher-uranium glass (Webb) based on conservative safety considerations. XRF sample preparation involved preparation by mixing approximately 1 g of sample with approximately 10 g of lithium tetraborate ($Li_2B_4O_7$) flux. The flux was doped with 0.5 wt% of lithium iodide (LiI) as a non-wetting (release) and anti-cracking agent. The mixture was melted to form a fused bead using a Claisse LeNeo Fused Bead maker, by melting in 5% Au–95% Pt casting bowls at 1065 °C, with rocking motions during melting and blown air during cooling. XRF data were collected with a PANalytical MagiX PRO XRF spectrometer (Malvern Panalytical Ltd., Malvern, UK) using a Rh anode X-ray tube. The XRF data were analysed using a modified version of the OXI program, a Wide Range Oxide XRF program based on many certified reference materials (CRM's), developed and verified internally [13]. The reader is referred to [13] for a full assessment of the detectors, accuracy and limits of detection associated with these measurements.

The SEM sample was prepared by mounting a piece of each glass onto a SEM stub using electrically-conductive silver paint, after which the samples were carbon coated in a carbon coater. Scanning Electron Microscopy (SEM) images and Electron Dispersive X-ray Spectroscopy (EDX) were carried out using a FEI Quanta3D FEG/FIB ESEM with AZtecLive software to provide EDX analysis in oxide wt%. The SEM-EDX results presented in Table 1 show an average of 4 analyses from different locations on the sample. The different numbers of decimal places quoted in the results in Table 1 reflect the relative accuracies of XRF and SEM-EDX analysis techniques, with conservative estimates of uncertainties associated with each technique shown in brackets. Results indicate that: (i) the Bagley Carnival glass is a soda-lime-silica type glass composition; and (ii) the Thomas Webb glass is a full English lead crystal type glass composition (Table 1).

Table 1. Analysed chemical compositions of Bagley and Webb glasses (conservative uncertainties shown in brackets).

Weight%	SiO_2	Al_2O_3	Na_2O	K_2O	MgO	CaO	CuO	PbO	As_2O_3	Sb_2O_3	U_3O_8
Bagley Carnival (XRF)	69.83 (±1.5)	1.71 (±0.2)	18.64 (±1)	1.83 (±0.2)	<l.d.	6.34 (±0.5)	<l.d.	<l.d.	1.38 (±0.2)	<l.d.	0.27 (±0.1)
Thomas Webb (SEM-EDX)	49.9 (±5)	<l.d.	<l.d.	9.0 (±1)	<l.d.	<l.d.	<l.d.	36.8 (±4)	<l.d.	2.8 (±0.5)	1.5 (±0.5)

<l.d., below limit of detection

Optical absorption spectra were obtained in transmission mode using a double beam computerized Perkin-Elmer Lambda 1050 spectrophotometer. The spectral resolution varies from 0.8 nm in the UV region to 2 nm in the near IR - visible region. After correction for reflection, the absorption spectra were normalized to sample thickness.

X-ray absorption spectra (XAS) were measured at the MARS beamline at the SOLEIL synchrotron (Saint-Aubin, France). The storage ring was operating in top-up mode at an electron current of 450 mA, 2.5 GeV. High-energy resolution fluorescence-detected XANES (HERFD-XANES) spectra were measured at the U M_4-edge (3.7 keV) using a double crystal monochromator (DCM) with a pair of Si(111) crystals. Higher harmonics rejection and vertical focusing was achieved using the Si strip of two mirrors inserted before and after the DCM with a 4 mrad incidence angle. The incident energy was calibrated using the absorption K-edge of potassium in a KBr pellet (3.614 keV).

EPR spectra were recorded at X-band (9.4 GHz) using a Bruker EMXplus spectrometer equipped with a high-sensitivity cavity. The measurements were performed at room temperature with a 100 kHz frequency modulation and 40 mW microwave power. Low temperature measurements were carried out using an Oxford cryostat allowing measurements down to 77K. A magnetic field modulation of 1 and 0.15 mT was used for a full spectrum acquisition and for the central spectral region of the EPR spectra, respectively. The data interval was 0.02 mT in this central zone. The spectra were measured in calibrated silica tubes (Suprasil grade). EPR signals are characterized by effective *g*-factor values defined by the resonance condition:

$h\nu = g\beta H$

where h is the Planck constant, ν the microwave frequency, ß the Bohr magneton and H the magnetic field. The DPPH standard (g = 2.0036) is used to calibrate g values.

4. RESULTS

4.1. Glass compositions

Chemical analyses shown in Table 1 have confirmed that the Bagley glass is a relatively high-sodium SiO_2-Na_2O-CaO glass, also containing Al_2O_3 and K_2O. The high (~20.5 weight %) alkali oxide content would have enabled lower melting temperatures and easier forming by comparison with modern commercial SiO_2-Na_2O-CaO glasses. The Bagley glass contains 0.27 weight% U_3O_8 equivalent, and was refined and oxidised by the presence in the batch of arsenic oxide (~1.4 weight% As_2O_3), presumably combined with nitrate additions [14,15].

The Thomas Webb glass composition confirms (Table 1) that it is a SiO_2-K_2O-PbO glass that can be described as English full lead crystal (it contains 36.8 weight % PbO, comfortably above the 30 weight % PbO threshold required to qualify as full lead crystal). The Webb glass contains 1.5 weight % U_3O_8 equivalent, and was refined by antimony oxide (2.8 weight % Sb_2O_3), presumably combined with nitrate batch additions [14,15]. The considerably higher uranium content of the Webb glass compared to the Bagley glass, first identified visually and also in terms of radioactivity (see Section 4.2.), is thus confirmed by XRF and SEM-EDX analyses. Indeed, a uranium content of 1.5 weight % is considered high from a historical uranium glass perspective, within the highest ~10% of uranium contents based on nearly 500 surveyed uranium glass articles [16].

Based on the measured chemical compositions, a search of relevant literature suggests that the glass transition temperatures, T_g, for both the Bagley and Webb glasses, were no greater than 500^{o}C [17,18]. Consequently it may be assumed that the heat treatments undertaken here at 550^{o}C were at temperatures above T_g for both glasses, and consequently whilst, at only a few tens of degrees Celsius above T_g for these commercial glasses, crystallization rates could reasonably be expected to be so slow as to be close to negligible, any mutual redox interactions between different multivalent ions in the glass for which a thermodynamic driver exists may, on the other hand, be able to proceed – albeit slowly - under such conditions [19].

4.2. Radioactivity of the two glasses

The Webb Glass sample measured a max of 2.0 μSv h^{-1} and the Bagley glass 0.5 μSv h^{-1}. The beta dose measurements made on another Bagley Carnival green glass [16] indicate 3

μSvh^{-1}. From a publication of the Health Protection Agency (HPA) the average background in the UK is 0.3108 $\mu Sv\ h^{-1}$ [20]. Similarly, in France, natural irradiation doses may reach 0.349 μSvh^{-1} in specific geological contexts [21]. Both samples (one only slightly above background) recorded values above background but well within one order of magnitude of background. These glasses do not require special handling due to radiation levels lower than required by regulations and are suitable for sending via Royal Mail [16].

4.3. UV-Visible-NIR optical absorption spectroscopy

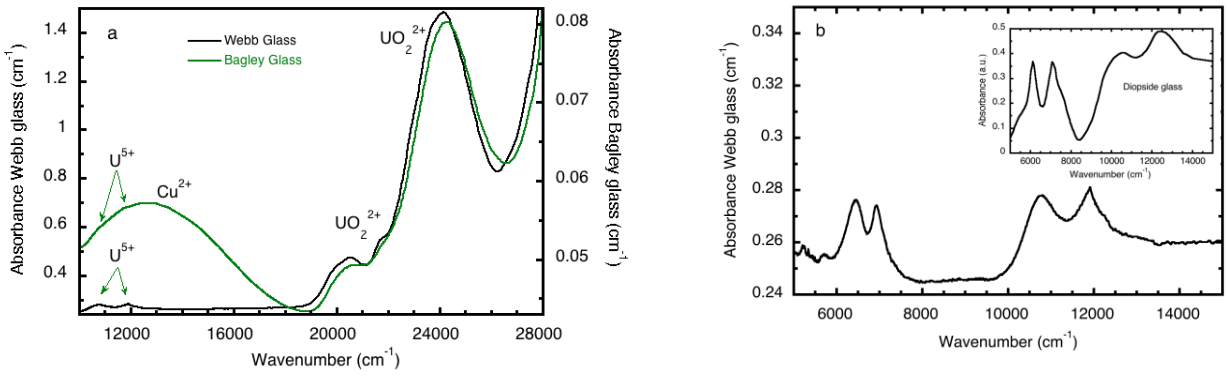

Figure 2. Optical absorption spectra of the Bagley and Webb glasses. (a) Comparison between the two samples after normalizing to the same apparent intensity of the uranyl groups to compare the relative concentration of U(V). The spectrum of the Webb glass exhibits the absorption bands of both uranyl and pentavalent uranium. The spectrum of the Bagley glass exhibits absorption bands of uranyl and pentavalent uranium and also Cu^{2+}. Superimposed absorption bands of U(V) (shown by arrows) have low intensity, close to the detection limit. (b) Absorption bands of U(V) in the Webb glass. Inset: Absorption spectrum, in the same spectral range, showing the absorption bands of U(V) in a uranium-containing $CaO\text{-}MgO\text{-}2SiO_2$ (diopside) glass (from [4], modified).

The optical absorption spectra of both Bagley and Webb glasses are compared in Fig. 2a. The spectra show the main absorption band of uranyl groups $(UO_2)^{2+}$ in the violet part of the optical spectra, near 24,200 cm^{-1}, as in other glasses [4,22]. In the Bagley glass, the presence of Cu^{2+} is characterized by an absorption band at 12,600 cm^{-1}. It was probably used to mimic, together with the uranyl contribution, the green U(IV) colour. The optical

spectrum characterizes Cu^{2+} in an octahedral site elongated by Jahn-Teller distortion [23,24], as observed in other historical glasses [25,26]. The position of these bands defines a transmission window near 19,000 cm^{-1} for the Bagley glass, at the origin of the green colour of this glass (Fig. 2a). The yellow colouration of the Webb glass is only due to the uranyl absorption bands in the violet part of the spectrum (Fig. 2b).

The contribution of U(V) is observed in the near infrared spectrum of the Webb glass at 6,430, 6,900, 10,700 and 11,900 cm^{-1} (Fig. 2b). These values are similar to those found in silicate and aluminosilicate glasses, at 6050, 7,070, 7,360, 10,050 and 11,900 cm^{-1} [4]. The U(V) absorption bands do not contribute to glass colouration. A contribution of U(V) is observed in the optical spectrum of the Bagley glass with features of low intensity near 10,700 and 11,900 cm^{-1}, superimposed to the broad absorption band of Cu^{2+}. This contribution of U(V) can be assessed to be about 10 times less intense relative to the uranyl contribution than in the Webb glass. This, in the context of the difference in uranium contents of the two glasses (by a factor of 5.5, see Table 1), therefore suggests that the U(VI) / U(V) ratio in the Bagley glass is greater than in the Webb glass. This difference indicates different redox conditions during glass elaboration (see § 4.3 on Uranium oxidation state in historical glasses). There is no evidence of U(IV) in either of the Webb or Bagley glasses. This oxidation state is characterized by three main absorption bands near 16,000, 9,100-9,800 and 5,500-5,700 cm^{-1} [4], the most intense being around 9,000 cm^{-1}, a region devoid of any absorption band in the glasses investigated (Fig. 2b).

Another difference between the spectroscopic properties of uranium in these glasses concerns the uranyl spectrum. The main absorption band occurs at 24,150 and 24,270 cm^{-1} in the Webb and the Bagley glass, respectively. These values are close to those found for the free uranyl ion, 24,140 cm^{-1}. This band splits under the low symmetry of the equatorial crystal field [27]. This may explain the origin of the splitting observed on the spectrum of the Webb glass at 23,750 and 24,150 cm^{-1}. Additional contributions occur at 19,900, 20,500 and 21,700 cm^{-1}, values close to what is observed in the absorption spectra of uranyl compounds. Their vibronic nature explains a relatively weak intensity at room temperature [28]. Site distribution effects result in the superposition of spectra from different uranyl sites, which is consistent with XANES-HERFD data. These distribution effects cause the broadening of the absorption bands that overlap [29]. This may give rise to the slight differences observed between the optical interacting uranyl spectra of the Webb and Bagley glasses, the former being more resolved than the latter. This may be caused by the distinct structure of soda-lime and lead crystal glasses. The absorption

spectra here investigated are in good agreement with those of uranophane ($Ca(UO_2)_2(SiO_3OH)_2 \cdot 5H_2O$), a crystalline uranyl silicate that can be considered as a reference material for silicate glasses. The main absorption band is split at 24,100 and 23,500 cm^{-1} and minor intensity bands occur at 21,300 and 20,400 cm^{-1} [29]. As in glasses, this spectrum does not exhibit well-defined uranyl vibronic bands. All these observations indicate a distinct uranyl surrounding in both of these glasses, particularly given their substantially different chemical compositions (Table 1).

4.4. HERFD-XANES

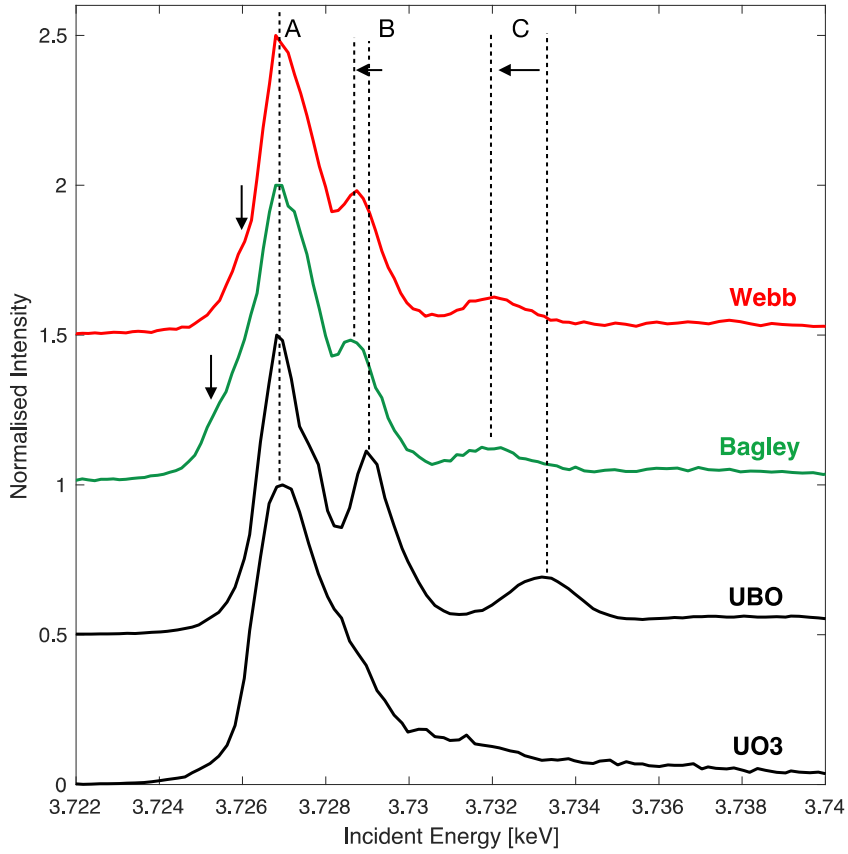

Figure 3. U M_4-edge HERFD XANES spectra of uranium in Thomas Webb glass Bagley glass compared to UO_2^{2+} references: uranyl borate (UBO) [30] and UO_3 uranate [31]. The intensity scale has been normalized to the maximum of the white line. The shoulders denoted by arrows indicate the presence of minority reduced U-species in the two glasses.

HERFD-XANES is a choice method to determine uranium speciation in glasses [32]. As it is obtained by measuring the Mβ emission, the effect of core-hole broadening is

reduced, which allows unambiguously determining the oxidation state of U ions [32]. The position of the white line A (Fig. 3) indicates the U oxidation state [32]. Comparison with crystalline references confirms that U is mostly hexavalent in both the Thomas Webb and Bagley glasses. In both glasses, we observe a weak shoulder on the low energy side of the white line (A), which can be assigned to the presence of small amounts of reduced uranium [9,31,33]. These results are consistent with the presence of uranium mostly as UO_2^{2+} with a possible small amount of U(V) as shown by U-M_4 HR-XANES in silicate glasses synthetized in oxidizing or reducing conditions [9].

These data are consistent with our optical spectroscopy results. The three features observed in the U M_4-edge HERFD-XANES spectra are characteristic of the uranyl UO_2^{2+} speciation and correspond to the empty 5*f* levels split by the covalent uranyl bond. It has been shown recently that the position of feature C (and B) is a sensitive gauge of the geometry of the uranyl groups [30,34]. The downshift of 1 eV of the C transition indicates a change from 6 to 5-fold equatorial coordination in correlation with the increase of the two U-O_{ax} bond lengths as observed in glassy and crystalline borates [30,32]. This trend reflects a stabilization of the 5*f* empty levels and indicates a decrease of the uranyl bond covalence. Comparison with the reference spectra shows that the highest energy feature shifts also towards lower energy and that the white line is broader than in the crystalline uranyl reference. This suggests a distribution of hexavalent uranium between uranate and uranyl-type environments, as already observed in borosilicate glasses by time-resolved photoluminescence spectroscopy [12].

4.5. Electron Paramagnetic Resonance (EPR) Spectroscopy

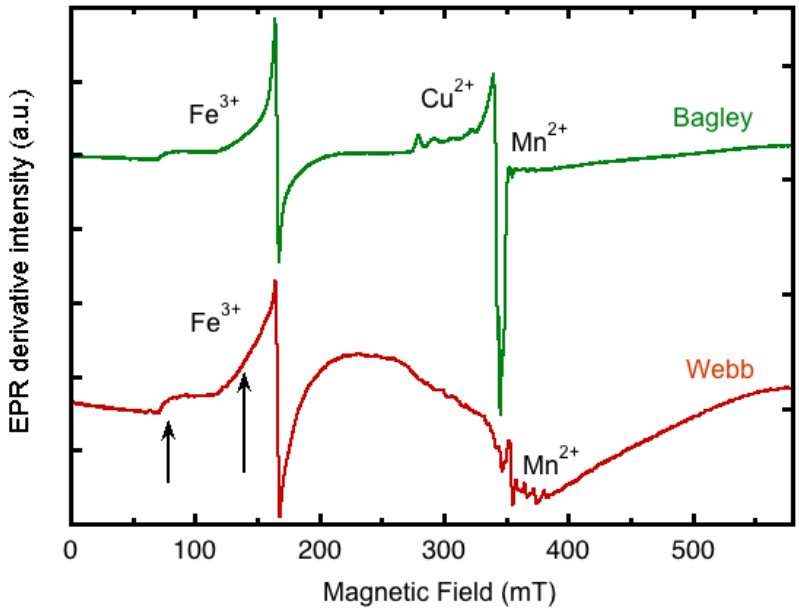

Figure 4. Electron Paramagnetic Resonance spectra of the Bagley (green) and Webb (red) glasses. The spectra have been normalized to the intensity of the Fe^{3+} signal near 165 mT. On the Webb spectrum, the arrows indicate the unusually large contribution of axially distorted Fe^{3+}sites near 75 and 140 mT.

EPR is a technique that is particularly sensitive to very (ppm) low concentrations of unpaired electrons, for example Fe^{3+}, Mn^{2+} or point defects such as hole centres. The EPR spectra of the two glasses studied here are notably different. The baseline is more complex in the spectrum for the Webb glass than for the Bagley glass, arising from a broad resonance centred near g=2 and extending over a wide range of magnetic fields (and clearly visible between 250 mT and 500 mT in Fig. 4). This resonance is attributed to magnetic interactions between clustered paramagnetic impurities, giving a superparamagnetic behaviour, as shown by a decreasing magnitude when measured at 100K (Fig. S2). In contrast, after heat treatment of the glass at 550°C for 12 hours, there is a strong, irreversible modification of this broad signal (Fig. S3) that may result from a structural evolution of the glass at high temperature. This is a good indication of molecular scale heterogeneity in the Webb glass, perhaps due to an insufficient fining time during melting.

The signals near 160 mT ($g \approx 4.3$) and 75 mT ($g \approx 8$) characterize isolated paramagnetic Fe^{3+} ions in rhombic and axially distorted sites, respectively. The shape of the Fe^{3+} EPR signal is not affected by external irradiation, as shown in silicate glasses containing 700 ppm Fe [35]. Such as the baseline, this signal is also different in the two glasses. However,

the peak-to-peak linewidth of the g ≈ 4.3 resonance, ΔH_{pp}, is the same (3.6 mT), within uncertainties, for both glasses. It has been shown that ΔH_{pp} for the Fe^{3+} $g \approx 4.3$ resonance increases linearly with increasing Fe^{3+} content in low-iron glasses [36]; however, glass composition-structure effects can also impact on ΔH_{pp} in silicate glasses with nominally the same Fe contents [37]. Therefore it may be concluded that the two glasses studied here, Bagley and Webb, contain similar (but not necessarily the same) ppm level Fe^{3+} contents.

For the Bagley glass, the $g \approx 4.3$ resonance in the EPR spectrum has the classical shape usually encountered for Fe^{3+} in glasses [38]. in the Webb glass, the unusual shape of this signal indicates the additional presence of Fe^{3+} sites presenting a smaller rhombic distortion and a concomitant larger axial distortion than usually encountered in Fe^{3+}-bearing glasses. These Fe^{3+} sites may be responsible for the additional contributions observed on the low field side of this resonance and for the relatively larger intensity of the $g \approx 8$ resonance (Fig. 4). The presence of two distinct Fe^{3+} sites may be evidence for the molecular scale heterogeneity of this glass. However, the intensity of this signal increases at low temperature, which is in accordance with the Curie law for paramagnetic ions.

After heating the Webb glass at 550°C for 12h and then re-measuring it, the intensity of the Fe^{3+} signal, and hence the fraction of paramagnetic Fe^{3+} increases. This modification may arise either from an oxidation of residual Fe^{2+} during heating at a temperature slightly above the glass transition temperature, T_g, or from a chemical diffusion of Fe^{3+} from superparamagnetic clusters. Whilst we have not measured T_g of the Webb glass, consideration of literature for compositionally-similar lead crystal glasses indicates a T_g of ≤ 500ºC [16,17].

Another possible cause of the observed increase in the $g \approx 4.3$ Fe^{3+} EPR signal in the Webb glass is a redox reaction involving the different redox-active species present, namely Sb, U and Fe. Since commercial glasses are rarely manufactured in such a way that they reach redox equilibrium, heating such a glass above its T_g as we have done can provide sufficient energy to drive redox reactions such as $Sb^{5+} + 2Fe^{2+} \rightarrow Sb^{3+} + 2Fe^{3+}$, which may have been driven to the right and could thus explain the apparent slight increase in Fe^{3+} content based on EPR data.

The intense signal observed in the Bagley glass in the region 300-350 mT arises from Cu^{2+}. This signal shows an anisotropic signal with four hyperfine components, characteristic of Cu^{2+}, with EPR parameters ($g_{//}$=2.35, $A_{//}$=142.10^{-4} cm^{-1}, $g_{\perp}$= 2.05,

$A_{\perp}$=22.10^{-4} cm^{-1}) similar to those observed in silicate glasses melted under oxidizing conditions [39]. This is consistent with an octahedral site with an axial distortion, in line with the optical data. Finally, the two glasses show a weak signal in the region 340-380 mT, with a hyperfine structure of six components characteristic of paramagnetic (diluted) $^{55}Mn^{2+}$. It is less intense in the Bagley than in the Webb glass. The intensity of the paramagnetic Mn^{2+} signal follows a Curie law at low temperature. As for Fe^{3+}, trace amounts of Mn^{2+} may come from the raw materials.

At higher resolution, annealing 12h at 550°C results in a complex modification of the spectra in the g = 2 region (Fig. 5). In addition to an intensification of the superparamagnetic signal, the intensity of the Mn^{2+} signal decreases. More important, the intensity of an incipient signal at 353 mT decreases, as shown in the difference EPR spectrum (Fig. S4). A similar signal, with an even lower intensity, is also observed in the Bagley glass. With a g-value of 2.005, slightly higher than that of free electron (g_e = 2.0024), and a linewidth of 1.5-1.8 mT, these defects may be related to the formation of positive holes, such as Non Bridging Oxygen Hole Centres (NBOHCs) or peroxy radicals (PORs). However, the low intensity of the defect signal at 353 mT, the presence of a complex baseline with superimposed signals from multivalent paramagnetic impurities (Fe^{3+}, Mn^{2+}, Cu^{2+}) together with the complex evolution of the spectra after annealing the Webb glass at 550°C for 12h preclude the full determination of the nature of this defect centre.

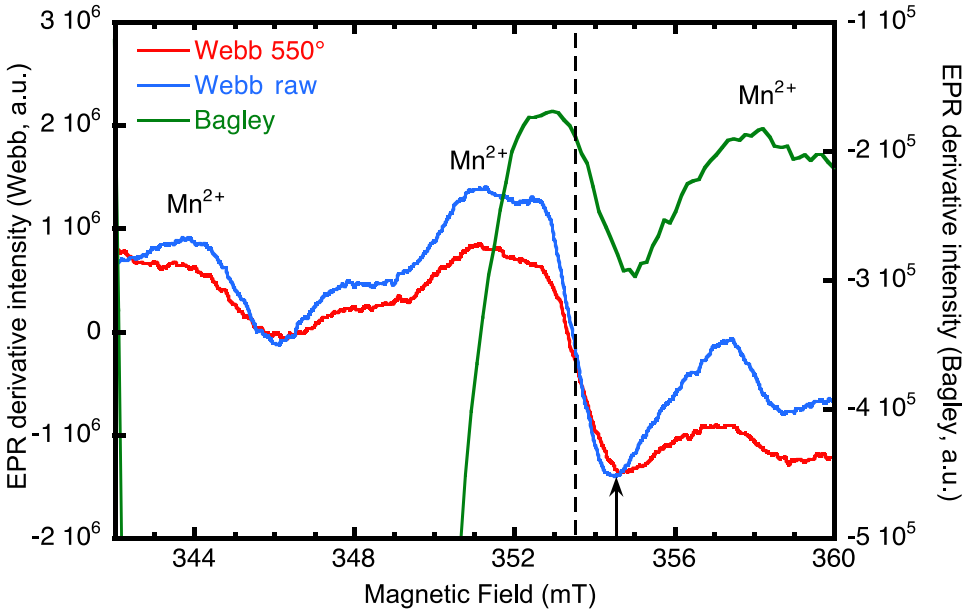

Figure 5. Detail of the central zone of the EPR spectra of the Webb and Bagley glasses. The signal at 353.5 mT in the Webb glass (dashed line) fits between two Mn^{2+} resonances and is slightly shifted in the Bagley glass, due to the proximity of the intense Cu^{2+} resonance at 342-352 mT. Its intensity decreases after the annealing treatment. The intensity of the Mn^{2+} resonances also decreases after annealing. The arrow indicates the position of the DPPH signal.

5. DISCUSSION

5.1. Colour of the Webb and Bagley historical glasses

Uranium glasses have been renowned for their original colours [40], encompassing dark green, yellow, yellow-green, orange, black and gray colours [3,5]. In particular, the green original and widely sought colour of historical glasses is not related to the presence of U (IV) in the Carnival (Bagley) glass. It is due to the presence of Cu^{2+} in addition to the uranyl groups, which impart a green hue additional to the yellow U(VI) colour. Concerning uranyl speciation, the U-absorption spectra of these glasses are in good agreement with those of uranophane ($Ca(UO_2)_2(SiO_3OH)_2 \cdot 5H_2O$), a bright yellow reference for uranyl-bearing silicate minerals. In addition to differences in colours, the depths (intensities) of the colours of the two glasses also differ considerably (Figure 1), with the Webb glass having a considerably stronger and deeper colouration than the Bagley glass. This can be attributed chiefly to different contents of colourants, with the Webb glass containing roughly a factor 6 more U_3O_8 than the Bagley glass (for which the CuO content was also below the limit of detection by XRF, as shown in Table 1). Figure 2 shows that the peak absorbance of the main visible absorption band, attributed to UO_2^{2+} ions, was ~0.08 cm^{-1} for the Bagley glass and ~1.5 cm^{-1} for the Webb glass. This difference in absorbance by about a factor 20 confirms that the differences in depth / intensity of colour between the two glasses can be primarily associated with differences in U_3O_8 content, with an additional contribution of the oxidizing conditions for the Webb glass.

5.2. Speciation of uranyl groups

The electronic structure of the uranyl ion can be described in terms of molecular orbitals formed by the unoccupied 5f and 6d valence orbitals of uranium and the 2s and 2p orbitals of the oxygen atoms. This σ overlap along the trans-dioxo bond allows electronic transitions by charge transfer from oxygen 2p to empty uranium 5f levels, at the origin of

the intense absorption in the violet spectral range. The main absorption band occurs at 24,150 and 24,270 cm^{-1} in the Webb and the Bagley glass, respectively. These values are close to those found for the free uranyl ion, 24,140 cm^{-1}. This intense transition is split under the low symmetry of the equatorial crystal field [27]. This may explain the origin of the splitting observed on the spectrum of the Webb glass at 23,750 and 24,150 cm^{-1}. A similar splitting of this band is also observed in uranophane, with maxima at 24,100 and 23,500 cm^{-1} [28].

Charge transfer transitions are coupled to the vibrational modes of the covalent uranyl group UO_2^{2+}, creating vibronic features superimposed to the optical transitions. However, in glasses, the structural disorder causes an inhomogeneous line broadening and the spectral structure of these weak vibronic transitions is not resolved at low temperature [41]. These weak transitions occur at 19,900, 20,500 and 21,700 cm^{-1}, values close to what is observed in the absorption spectra of uranyl compounds: e.g., minor bands occur at 21,300 and 20,400 cm^{-1} in uranophane [28]. Site distribution effects result in the superposition of spectra from different non-interacting uranyl groups and cause a broadening of the absorption bands that overlap [29]. Amorphous B_2O_3 is one of the few glasses to show a resolved vibronic structure of uranyl groups [42], probably because of the presence of rigid boroxol groups that improve the medium-range order around uranyl groups. These disorder effects give rise to the slight differences observed between the optical spectra of the Webb and Bagley glasses, which exhibit a resolved or unresolved splitting of the uranyl band, respectively. These differences may reflect the distinct medium-range structure of soda-lime and lead crystal glasses.

5.3. Uranium oxidation state in historical glasses

HERFD/XANES and optical absorption spectroscopy both demonstrate the presence of a small amount (not quantified) of U(V). The optical transitions of U(V), clearly visible in the spectrum for the Webb glass, are less intense in the Bagley spectrum (Figs. 2a and 2b). This shows that most U has been oxidized to U(VI) in the Bagley glass, probably because of the presence of both the Cu^{2+}/Cu^{+} redox couple and the As^{3+}/As^{5+} redox couple interacting with the U(V)/U(VI) redox couple (Fig. 5). The use of As (plus batch nitrate, presumably) as an oxidizing agent in the Bagley glass was clearly not sufficient to oxidise all uranium to U(VI). In soda-lime glasses, the relative reduction potential of the U(V)/U(VI) redox couple is higher than that of the Cu^{2+}/Cu^{+} redox couple, the latter being the electron acceptor as the former is the electron donor [43]. The optical transitions of

U(V) occur only in the near infrared and do not contribute to colouration. The addition of an oxidizing redox couple such as Cu^{2+}/Cu^{+} increases the glass colouring by U(VI). As the Fe^{3+}/Fe^{2+} redox couple may favour the formation of U(V), the colouration by uranyl groups is also favoured by a low Fe content of the glass (Fig. 6).

The redox potentials of the different redox couples present in the two glasses here are very important to the resulting glass redox. The Bagley glass contains at least five multivalent (and therefore redox-active) elements – U, As, Cu, Mn and Fe; whilst the Webb glass contains at least four – U, Sb, Mn and Fe. The contents of Cu, Mn and Fe are very small by comparison with U, As and / or Sb. The redox potentials developed by Schreiber et al. [43] for each redox couple in soda-lime-silica type glasses, are shown in Table 2. It may reasonably be assumed that whilst the values may differ between Bagley and Webb glasses, because of their compositional differences, the hierarchy / order of the potentials remains the same in both glasses, just as it does for aqueous solutions.

Table 2. Relative reduction potentials of selected redox couples in soda-lime-silica glass at 1400°C after [43]

Element	Redox Couple	Relative Reduction Potential *E'* (±0.3)
Mn	$Mn^{3+} \rightarrow Mn^{2+}$	+1.2
Sb	$Sb^{5+} \rightarrow Sb^{3+}$	+0.3
Cu	$Cu^{2+} \rightarrow Cu^{+}$	-0.2
U	$UO_2^{2+} \rightarrow U(V)$	-0.9
Fe	$Fe^{3+} \rightarrow Fe^{2+}$	-1.0
As	$As^{5+} \rightarrow As^{3+}$	-1.1

Appraisal of the redox potentials in Table 2 enables the explanation for the presence of the different species observed. For the Bagley glass, Mn would readily reduce to Mn^{2+}, as confirmed by EPR (Figs 4 and 5) whilst Fe would be expected to remain largely as Fe^{3+} and have little redox interaction with either U or As, because of their closely similar redox potentials. Moreover, the similarity in redox potentials between U and As (Table 2) may also have precluded strong redox interactions between the uranium and the oxidizing agent, arsenic. However, the low levels of Cu present in the glass do present a larger difference in redox potentials, so would interact to some degree with U, As and Fe to oxidise them

whilst itself reducing to form more Cu^{+}. Overall, it could be reasonably concluded that not all uranium is present as uranyl UO_2^{2+}, and that low levels of U(V), while not detected because of the low uranium content of the Bagley glass, cannot be ruled out, particularly in light of the above redox potentials. It should also be noted that, on the basis of redox potentials (Table 2). Arsenic oxide would be expected to perform poorly as an oxidizing agent in the Bagley glass, although more likely it was added to the batch as an oxidizing agent. As noted elsewhere [14,15,44], arsenic oxide has historically been widely used as an oxidizing agent in glass manufactures. However, it has also been shown [14,44] that As oxides are inferior in performance to Sb oxides as oxidizing agents in soda-lime-silica type glass melts.

For the Webb glass, a rather different redox situation arises, principally because of the greater oxidizing capability of Sb over As. As with the Bagley glass, the Mn would readily reduce to Mn^{2+}, as confirmed by EPR (Figs 4 and 5) and Fe would be expected to remain largely as Fe^{3+} with little redox interaction with U but considerable interaction with Sb, whereby the iron would be oxidized. The uranium would also be expected to interact strongly with Sb and become oxidized to uranyl UO_2^{2+}.

Qualifying which of the two glasses is more “oxidized” is challenging, given the available information. The Bagley glass clearly contains an inferior oxidizing agent (As), but the ratio of As_2O_3:U_3O_8 is high (~5). The Webb glass contains a superior oxidising agent (Sb) but the ratio of Sb_2O_3:U_3O_8 is lower (~2). Putting aside for a moment the additional, unquantified (and somewhat secondary) effects of differences in glass melt compositions and melting temperatures that undoubtedly arose between the Bagley and Webb glasses, it can thus be concluded that both glasses are reasonably oxidized, and the large majority of uranium in both glasses is uranyl UO_2^{2+}, as is supported by the available evidence from optical absorption spectroscopy and HERFD/XANES. The Webb glass definitively contains most uranium as uranyl UO_2^{2+} but with measurable level of U(V) and the Bagley glass contains most uranium as uranyl UO_2^{2+} and the possibility of low levels of U(V) cannot be discounted although it was not positively detected.

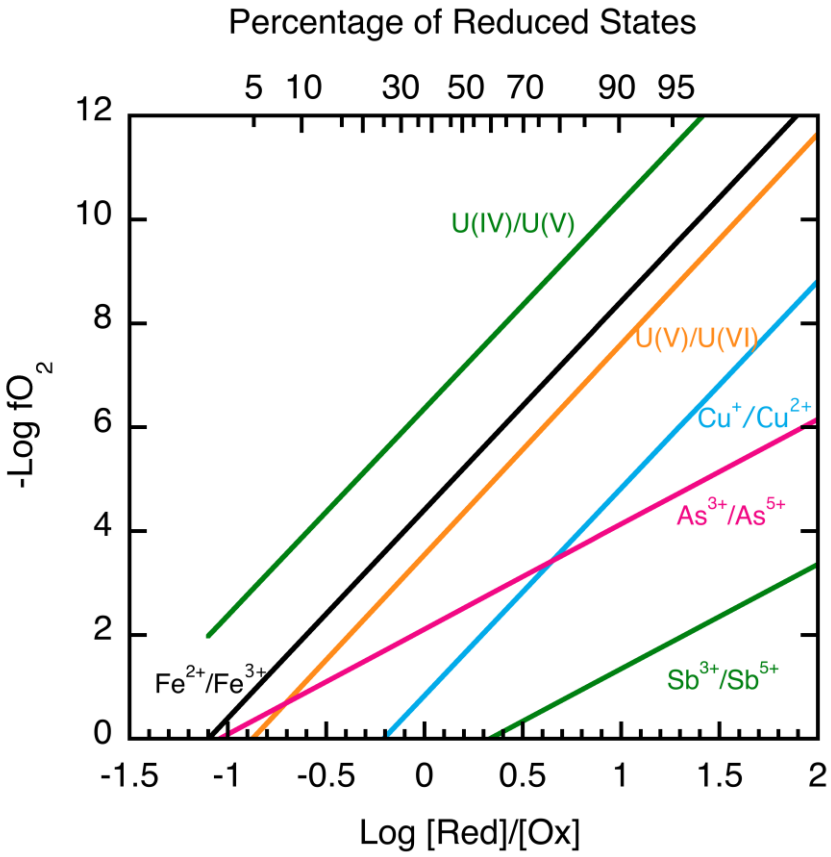

Figure 6. Evolution of redox ratios of multivalent elements in a soda-lime melt at 1400°C (after [43])

5.4. Does the presence of uranium give rise to radiation-induced damage?

Most optical absorption bands related to NBOHCs and other radiation centres occur at high wavenumbers [45,46] and give rise to shoulders superimposed to a sharp rising background. As a result, these absorption bands are hidden by the intense transitions of the uranyl groups. EPR is then the only technique giving information on the defect-related centres in these uranium glasses. However, the complex composition of these glasses brings with two limitations. First, the low concentration of these centres only gives rise to incipient signals, difficult to extract quantitatively from the complex baseline where several other EPR signals coexist. The same signal at 353 mT is observed in both Bagley and Webb glasses, but its intensity is smaller in the former than in the latter, in relation with a smaller U content of the Bagley glass. Second, thermal annealing experiments able to investigate defect centres show irreversible modifications of the EPR spectra in the Webb glass heated at 550°C for 12h. The changes are many: modification of the intensity of the signals from multivalent elements (Mn, Fe, Cu) and changes in the shape and

intensity of the broad signal at about g=2. In addition, the role of Sb on U-oxidation state is unknown but expected to be non-zero.

The low intensity of the incipient signal tentatively assigned to radiation defect centres may be explained by a partial trapping of electrons and holes by the multivalent impurities present in the glass, as Fe, Mn, Cu, As or Sb, and U. Several studies have shown such self-healing or radiation-hard behaviour in glasses containing multivalent elements [47-50]. In the specific case of self-irradiation in glasses, the radioactive decay generates excitons that interact with the redox couples present. This may explain the modification of the intensity of the absorption by paramagnetic impurities after glass annealing. Such processes were evocated to explain the reduced sensitivity of nuclear glasses to ionizing radiation [51] as compared to glasses devoid of transition elements. Recent research by some of the present authors [50] has shown that the presence of Sb in glass can improve radiation-hardness of the glass and greatly reduce the number of defect centres caused by gamma-irradiation. Broadly similar behaviour from As could also reasonably be expected. A key aspect of the behaviour of Sb was to form low levels of the rare oxidation state, Sb^{4+}, as detected by EPR [52]. Interestingly, no Sb^{4+} EPR signal is detected for the Webb glass studied here, suggesting that if any Sb^{4+} were present then it exists only at very low levels.

The radiation dose suffered by the glasses will also depend on how old they are. In the glasses made with synthetic uranium chemicals, the radioactivity comes from ^{238}U and its decay product, ^{234}U, both at 49% by activity and ^{235}U being at 2% by activity. The long half-life of ^{238}U ($4.5\ 10^9$ yrs.) can be considered not to cause significant activities to glasses with a moderate U-content. According to [16], the annual skin dose to the hands would be about 100 μ Sv by spending the equivalent of one day a year (7 h) handling a uranium glass made for decorative purposes. For the Bagley and Webb glasses, the annual dose received under these conditions would be 21 and 70 µSv, respectively, using the dose rate given in 3.1. This is well below the 1 mSv annual effective dose equivalent limit for a member of the public [53] and even lower than the radiation dose suffered during a round trip from Europe to Japan or California, evaluated at about 150 µSv [54]. Such a low activity may explain a limited efficiency for creating stable radiation centres in these not too old glasses. At the same time, the low activity shows that there is no danger for such glasses to be exhibited in museums.

6. CONCLUSION

Although uranium has been extensively used to create original colours of glasses, glazes and enamels between the 1830s and 1940s, these materials have not been extensively investigated. Among the topics of interest are the origin of the colouration and the impact of the radioactivity arising from the presence of uranium. This work is the first detailed study of these historical glasses showing the interest of associating data on chemical composition and uranium speciation to determine the specific elaboration conditions of these glasses. In particular, the presence of minority U(V) is confirmed by optical absorption spectroscopy and High-Energy Resolution Fluorescence-Detected (HERFD)-XANES. These original data on the redox state of uranium provide constraints on the techniques used for oxidizing the glass. Finally their low radioactivity is at the origin of the presence of incipient radiation defects, but it remains well below the annual effective dose equivalent limit recommended for the public.

Acknowledgements

The authors thank A. M. T. Bell and F. Sweeney for training and assistance with the XRF and SEM-EDX analyses.

REFERENCES

[1] L. Cartechini, C. Miliani, L. Nodari, F. Rosi, P. Tomasin, The chemistry of making color in art. J. Cult. Herit. 50 (2021) 188−210.

[2] R. Procházka, V. Ettler, V. Goliáš, M. Klementová, M. Mihaljevič, O. Šebek, L. Strnad, A comparison of natural and experimental long-term corrosion of uranium-coloured glass. J. Non-Cryst. Solids 355 (2009) 2134-2142.

[3] F. Lopes, A. Ruivo, V.S.F. Muralha, A. Lima, P. Duarte, I. Paiva, A. Pires de Matos, Uranium glass in museum collections. J. Cult. Herit. 9 (2008) e64-e68.

[4] G. Calas, Etude expérimentale du comportement de l'uranium dans les magmas: États d'oxydation et coordinance. Geochim. Cosmochim. Acta 43 (1979)1521-1531.

[5] D. Strahan, Uranium in glass, glazes and enamels: history, identification and handling. Stud. Conserv. 46 (2001) 181-195.

[6] R.N. Mutafela, J. Mantero, Y. Jani, R. Thomas, E. Holm, W. Hogland, Radiometrical and physico-chemical characterisation of contaminated glass waste from a glass dump in Sweden. Chemosph. 241 (2020) 124964.

[7] Y.L. Liu, M.H. Huo, S.Z. Ruan, K.J. Su, W.Y. Zhang, L. Jiao, EPR dosimetric properties of different window glasses. Nucl. Instrum. Methods Phys. Res. B 443 (2019) 5-14.

[8] S.W.S. McKeever, S. Sholom, J.R. Chandler, A comparative study of EPR and TL signals in Gorilla© Glass. Radiat. Protect. Dosim. 186 (2019) 65–69.

[9] P. Chevreux, L. Tissandier, A. Laplace, T. Vitova, S. Bahl, F. Le Guyadec, E. Deloule, Uranium solubility and speciation in reductive soda-lime aluminosilicate glass melts. J. Nucl. Mater. 544 (2021) 152666.

[10] A.J. Connelly, N.C. Hyatt, K.P. Travis, R.J. Hand, M.C. Stennett, A.S. Gandy, A.P. Brown, D.C. Apperley, The effect of uranium oxide additions on the structure of alkali borosilicate glasses. J. Non-Cryst. Solids. 378 (2013) 282-289.

[11] M. Mohapatra, R.M. Kadam, S.V. Godbole, R.K. Mishra, C.P. Kaushik, B.S. Tomar, Gamma radiation-induced changes in Trombay nuclear waste glass containing iron. Int. J. Appl. Glass Sci.4 (2013) 53-60.

[12] N. Ollier, M.J. Guittet, M. Gautier‑Soyer, G. Panczer, B. Champagnon, P. Jollivet, U environment in leached SON68 type glass: a coupled XPS and time-resolved photoluminescence spectroscopy study. Opt. Mater. 24 (2003) 63-68.

[13] A.M.T. Bell, D.J. Backhouse, W. Deng, J.D. Eales, E. Kilinc, K. Love, P. Rautiyal, J.C. Rigby, A.H. Stone, S. Vaishnav, G. Wie-Addo, P.A. Bingham PA, X-ray

fluorescence analysis of feldspars and silicate glass: Effects of melting time on fused bead consistency and volatilisation. Minerals 10 (2020), 442.
[14] J.E. Shelby, Introduction to glass science and technology, 2nd Ed. Royal Soc. Chem. (2005), London, UK.
[15] C. Stålhandske, Refining of lead glass using As(III)/Sb(III) or As(V)/SB(V). Glastek. Tidskr. 54 (1999) 87-92.
[16] S.J. Watson, J.S. Hughes, Radiological implications of the use of uranium in Vaseline glass. J. Radiol. Prot. 30 (2010) 535–544.
[17] M.B. Volf, Technical Glasses. Isaac Pitman & Sons, London (1961).
[18] M.B. Volf, Technical approach to glass. Elsevier, Amsterdam (1990).
[19] A. Paul, Chemistry of Glasses, 2nd Ed. Chapman & Hall, London (1990.
[20] Health Protection Agency, https://assets.publishing.service.gov.uk/government/uploads/system/uploads/attachment_data/file/340209/HpaRpd001.pdf (2005).
[21] E. Warnery, G. Ielsch, C. Lajaunie, E. Cale, H. Wackernagel, C. Debayle, J. Guillevic, Indoor terrestrial gamma dose rate mapping in France: a case study using two different geostatistical models. J. Environ. Radioact. 139 (2015) 140-148.
[22] A.F. Leung, T.W. Lai, Spectral analysis and kinetics of uranyl glasses. J. Chem. Phys. 76 (1982) 3913-3920.
[23] L.G. Bäck, Electronic spectra and molar extinction coefficient of Cu^{2+} in mixed alkali–alkaline earth–silica glasses. Phys. Chem. Glasses: Eur. J. Glass Sci. Technol. B. 56 (2015) 8-14.
[24] M. Cable, Z.D. Xiang, The optical spectra of copper ions in alkali-lime-silica glasses. Phys. Chem. Glasses 33 (1992) 154-160.
[25] N. Capobianco, M.O.J.Y. Hunault, S. Balcon-Berry, L. Galoisy, D. Sandron, G. Calas, The Grande rose of the Reims Cathedral: an eight-century perspective on the colour management of medieval stained glass. Sci Rep. 9 (2019) 3287.
[26] M.O.J.Y. Hunault, C. Loisel, Looking through model medieval green glasses: From colour to recipe. Int. J. Appl. Glass Sci. 11 (2020) 463-470.
[27] P. Nockemann, K. Servaes, R. Van Deun, K. Van Hecke, L. Van Meervelt, K. Binnemans, C. Görller-Walrand, Speciation of uranyl complexes in ionic liquids by optical spectroscopy. Inorg. Chem. 46 (2007) 11335– 11344,

[28] J.P. deNeufville, A. Kasdan, R.J.L. Chimenti, Selective detection of uranium by laser-induced fluorescence: a potential remote-sensing technique. 1: Optical characteristics of uranyl geologic targets. Appl. Optics 20 (1981) 1279–1296.
[29] K.L. Lam, A.F. Leung, Energy Spectrum of Uranyl Ions in Soda-Lime Glass. J. Non-Cryst. Solids, 23 (1977) 385-400.
[30] M.O.J.Y. Hunault, D. Menut, O. Tougait, Alkali uranyl borates: bond length, equatorial coordination and 5f states. Crystals 11 (2021) 56.
[31] R. Bès, K. Kvashnina, A. Rossberg, G. Dottavio, L. Desgranges, Y. Pontillon, P. Solari, S. Butorin, P. Martin, New insight in the uranium valence state determination in $U_yNd_{1-y}O_{2\pm x}$. J. Nucl. Mater. 507 (2018) 145–150.
[32] M.O.J.Y. Hunault, G. Lelong, L. Cormier, L. Galoisy, P. Solari, G. Calas, Speciation change of uranyl in lithium borate glasses. Inorg. Chem. 58 (2019) 6858–6865.
[33] G Leinders, R Bes, J Pakarinen, K Kvashnina, M. Verwerft, Evolution of the uranium chemical state in mixed-valence oxides, Inorg. Chem. 56 (2017) 6784–6787.
[34] L. Amidani, M. Retegan, A. Volkova, K. Popa, P.M. Martin, K.O. Kvashnina, Probing the local coordination of hexavalent uranium and the splitting of 5f orbitals induced by chemical bonding, Inorg. Chem. 60 (2021), 16286–16293.
[35] K. Kadono, N. Itakura, T. Akai, M. Yamashita, T. Yazawa, Effects of iron on the formation and annihilation of X-ray irradiation induced non-bridging oxygen hole centers in soda-lime silicate glass. J. Non-Cryst. Solids 356 (2010) 232-235.
[36] S.K. Mendiratta, E.G. De Sousa, Clustering and g = 4.3 ESR peak in iron-containing glasses, J. Mat. Sci. Lett. 7 (1988) 733-734.
[37] P.A. Bingham, The environment of iron in silicate glasses, PhD thesis, University of Sheffield, UK, (2000)
[38] V. Vercamer, G. Lelong, H. Hijiya, Y. Kondo, L. Galoisy, G. Calas, Diluted Fe in silicate glasses: structural effects of Fe-redox state and matrix composition. An optical absorption and X-band/ Q-band EPR study. J. Non-Cryst. Solids 428 (2015) 138–145.
[39] L.D. Bogomolova, A.G. Fedorov, V.A. Jachkin, V.N. Lazukin, EPR and optical spectra of gamma-irradiated sodium-silicate glasses containing copper oxide. J. Non-Cryst. Solids 37 (1980) 381-386,
[40] F. Lole, Notes: uranium glass in 1817—A Pre-Riedel Record. J. Glass Studies 37 (1995)139-140.

[41] K. Binnemans, H. De Leebeeck, C. Görller-Walrand, J.L. Adam, Spectroscopic properties of uranyl ions in fluorophosphate glasses. J. Phys. Condens. Matter. 11 (1999) 4283–4287.

[42] G.K. Liu, V.S. Vikhnin, H.Z. Zhuang, K.S. Hong, J.V. Beitz, M.R. Antonio, L. Soderholm, C.W. Williams, Formation of $UO_2(BO_3)_4$ clusters in B_2O_3 glass due to charge transfer and vibronic effects. J. Lumin. 94 (2001) 677-681.

[43] H.D. Schreiber, N.R. Wilk Jr, C.W. Schreiber, A comprehensive electromotive force series of redox couples in soda-lime-silicate glass. J. Non-Cryst. Solids. 253 (1999) 68-75.

[44] M. Cable, A.A. Naqvi, The refining of a soda-lime-silica glass with antimony. Glass Technol. 16 (1975) 2-11.

[45] K. Farah, M. Arbi, F. Hosni, A.H. Hamzaoui, B. Boizot, Formation and decay of colour centres in silicate glasses exposed to gamma radiation: Application to high-dose dosimetry. *Current Topics in Ionizing Radiation Research*, ed., M. Nenoi. InTech, Open access, Shanghai, China (2012) 603–624.

[46] P. Rautiyal, G. Gupta, R. Edge, L. Leay, A. Daubney, M. Patel, A. Jone, P.A. Bingham, Gamma irradiation-induced defects in borosilicate glasses for high-level radioactive waste immobilisation. J. Nucl. Mater. 544 (2020) 152702.

[47] B. Boizot, G. Petite, D. Ghaleb, G. Calas, Dose, dose rate and irradiation temperature effects in β-irradiated simplified nuclear waste glasses by EPR spectroscopy. J. Non-Cryst. Solids. 283 (2001) 179-185.

[48] E. Malchukova, B. Boizot, G. Petite, D. Ghaleb, Irradiation effects in oxide glasses doped with transition and rare-earth elements. Eur. Phys. J. Appl. Phys. 45 (2009) 10701.

[49] O.J. McGann, P.A. Bingham, R.J. Hand, A.S. Gandy, M. Kavcic, M Zitnik, K. Bucar, R. Edge, N.C. Hyatt, The effects of gamma-radiation on model vitreous wasteforms intended for the disposal of intermediate and high level radioactive wastes in the United Kingdom. J. Nucl. Mater. 429 (2012) 353.

[50] G. Gupta, T.Y. Chen, P. Rautiyal, A.G. Williams, A.W. Evan, S. Kamali, J.A. Johnson, C.E. Johnson, R. Edge, P.A. Bingham, Antimony-modified soda-lime-silica glass: towards low-cost radiation-resistant materials, J. Non-Cryst. Solids (under review, 2022).

[51] A.H. Mir, S. Peuget, External ion irradiations for simulating self-irradiation damage in nuclear waste glasses: State of the art, recommendations and prospects. J. Nucl. Mater. 539 (2020) 152246.

[52] J.W.H. Schreurs, D.H. Davis, EPR spectrum of Sb^{4+} in a silicate glass. J. Chem. Phys. 71 (1979) 557-559.

[53] US Nuclear Regulatory Commission (2001) Systematic radiological assessment of exemptions for source and by-product materials (NUREG-1717) (Washington, US Nuclear Regulatory Commission Office of Nuclear Regulatory Research)

[54] J.F. Bottollier-Depois, Q. Chau, P. Bouisset, G. Kerlau, L. Plawinski, L. Lebaron-Jacobs, Assessing exposure to cosmic radiation on board aircraft. Adv. Space Res. 32 (2003) 59–66.

Supplemental information

Spectroscopic investigation of historical uranium glasses

Georges Calas[1], Laurence Galoisy[1], Myrtille Hunault[2], Prince Rautiyal[3], Katrina Skerratt-Love[3], Jessica Rigby[3], Paul A. Bingham[3]

[1] Institut de Minéralogie, de Physique des Matériaux et de Cosmochimie (IMPMC), Sorbonne Université, CNRS, Muséum National d'Histoire Naturelle, IRD, 75005 Paris, France

[2] Synchrotron SOLEIL, L'Orme des Merisiers, Saint Aubin BP 48, 91192 Gif-sur-Yvette, France

[3] Materials and Engineering Research Institute (MERI), Sheffield Hallam University, City Campus, Howard Street, Sheffield S1 1WB, UK

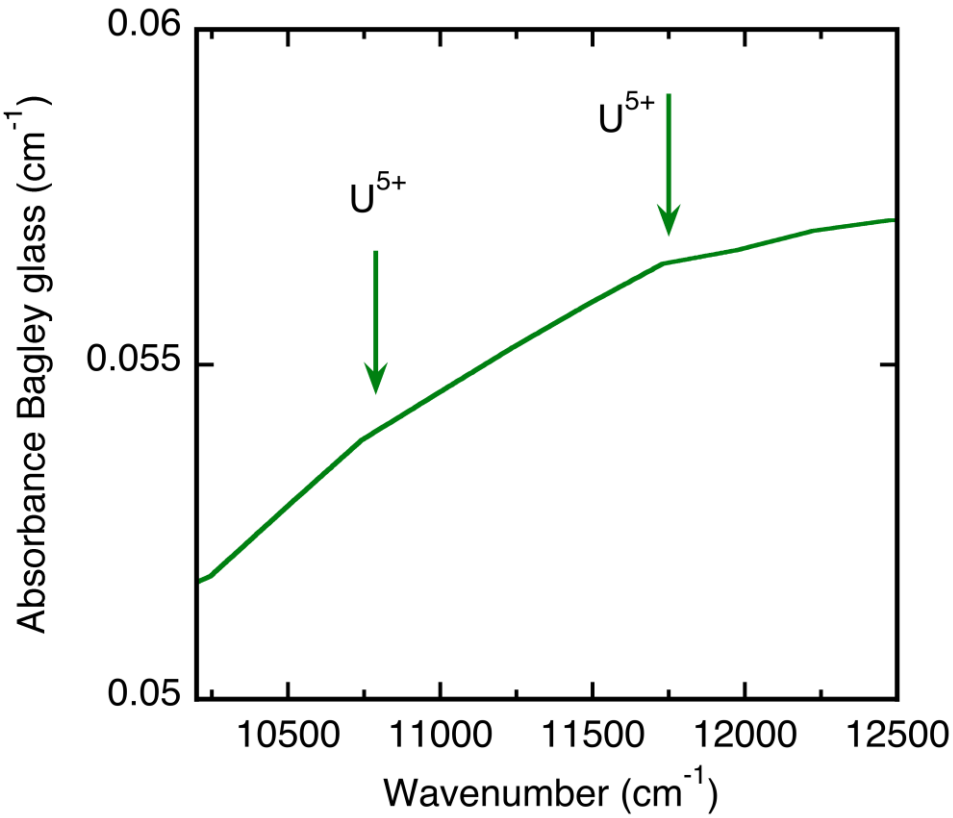

Figure S1. Detail of the optical transitions of U(V) in the Bagley glass.

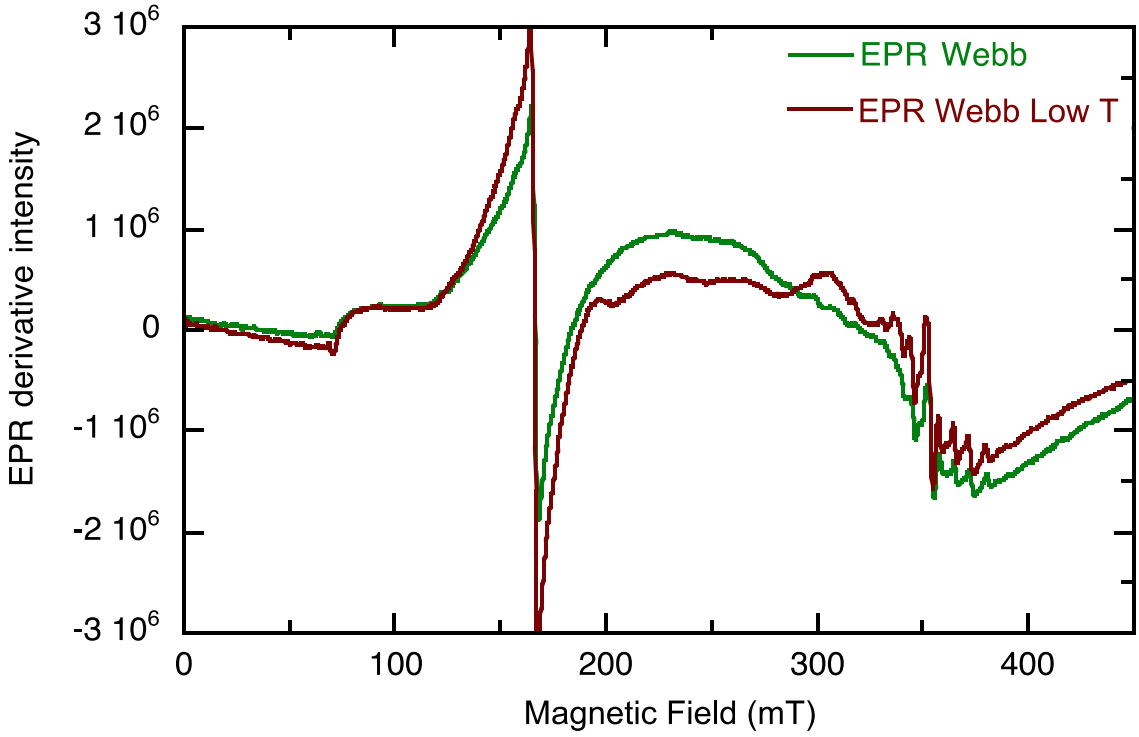

Figure S2. EPR spectrum of the Webb glass at ambiant and low temperature.

The spectra have been recorded on the same sample and may be quantitatively compared. They show a decrease of the broad signal due to magnetic couplings, showing their superparamagnetic nature. At the same time, there is an increase of the intensity of the Fe^{3+} and Mn^{2+} resonances, following the Curie law for paramagnetic ions.

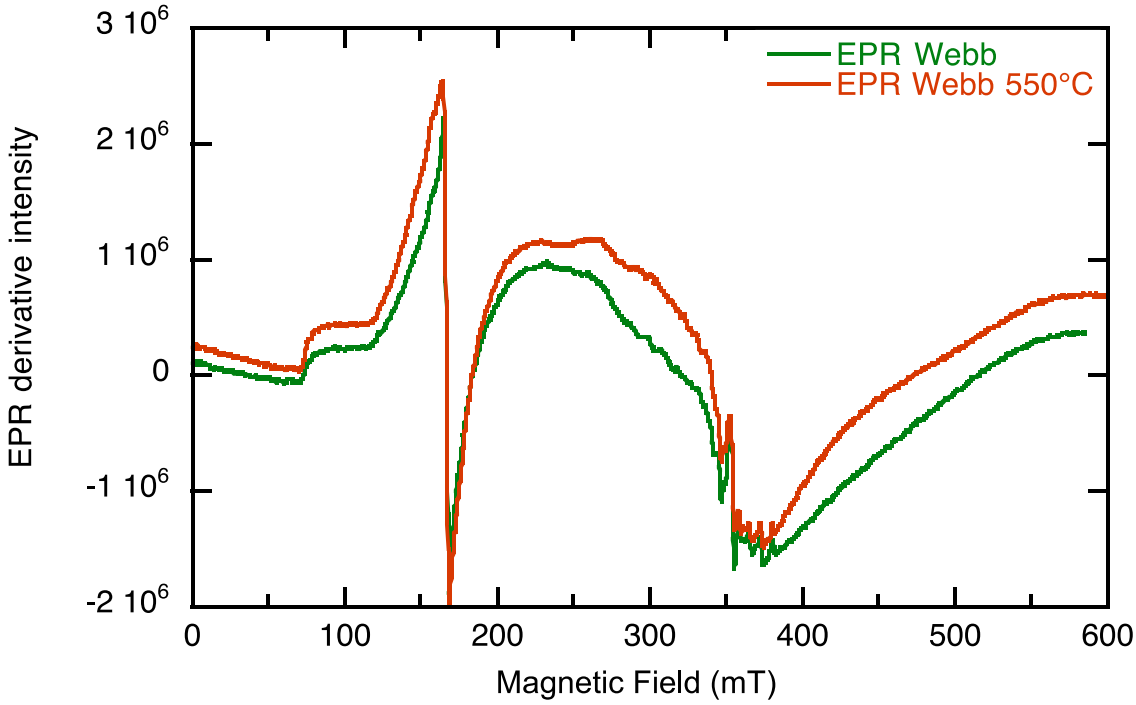

Figure S3. EPR spectrum of the Webb glass before and after annealing at 550°C during 12h.

The spectra have been recorded on the same sample and may be quantitatively compared. They show a strong, irreversible modification of the broad baseline, as a result of the structural evolution of the glass at high temperature, an indication of some chemical heterogeneity. The Fe^{3+} resonance also increases irreversibly, showing a larger fraction of paramagnetic Fe^{3+}.

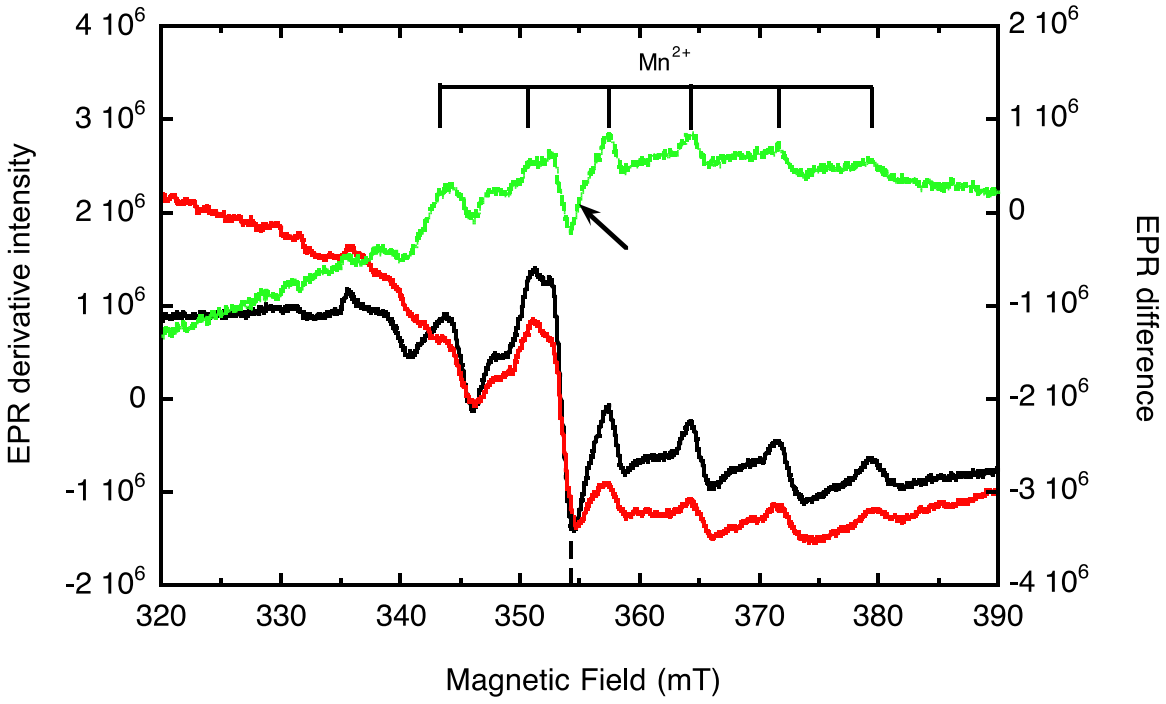

Figure S4. Central zone of the EPR spectra of the pristine Webb glass (blue curve, top) and after annealing 12h at 550°C (black curve, bottom). The position of the DPPH calibrant (g=2.0036) in indicated by the dashed line at the bottom. The EPR difference spectrum shows the disappearance of an asymmetric signal (indicated by an arrow), at g values slightly larger than the DPPH value.